# Data-driven aerodynamic models for reduced-order aeroelastic simulations

Dávid András Horváth, János Lelkes
*Budapest University of Technology and Economics, Faculty of Mechanical Engineering, Department of Fluid Dynamics, Budapest, Hungary*

*Summary*. Time-dependent aerodynamic loads of thin elastic structures subjected to airflow can be calculated by numerous methods. Analytical, semi-empirical, reduced-order, and CFD-based models can be utilized to calculate the aerodynamic loads. Calculations of the aerodynamic loads are influenced by nonlinear aerodynamic effects for large deformations of the elastic structure, such as dynamic stall, hysteresis, and vortex formation. In this work, the applicability and accuracy of a data-based identification method for calculating the aerodynamic loads in the time domain are investigated. To create the data-based model, high precision validated CFD simulations were used. The model was constructed using the SINDy (Sparse Identification of Nonlinear Dynamics) algorithm. After the initial data fitting process, the reduced-order aeroelastic simulations with the identified aerodynamic models run up to five magnitudes faster than classical high precision FSI simulations. The most significant advantage of this method is that it can be applied to a large variety of different geometries, and it is also accurate for large deformations and large angles of attack in the nonlinear aerodynamic regime.

## Introduction

Obtaining accurate and efficient aerodynamic models has been a fundamental goal of research efforts in aeronautics over the past century [1]. Aerodynamic models are essential for designing aircrafts [2], building large span elastic bridges [3]. Accurate aerodynamic models are used to evaluate static and dynamic aeroelastic stability and develop feedback control laws for aircraft. Closed-form solutions for the attached incompressible unsteady flow problem around a two-dimensional (2D) airfoil exist in both the frequency and time domains [4]. However, these models do not provide acceptable results in the case of rapid oscillations and high angles of attack.

Semi-empirical models such as ONERA and Leishman-Beddoes can be used to approximate the aerodynamic nonlinearity caused by the dynamic stall and flow separation. Lelkes and Kalmár-Nagy modeled the aerodynamic forces for large angles of attack as a piecewise linear function, which was able to capture the phenomenon of dynamic stall [5].

Considering machine learning advancements, developing reduced-order models based on data obtained from measurements or numerical simulations began to gain popularity recently [6]. An overview of data-driven methods in aerospace engineering is given by Brunton et al. [7]. In the work of Pohl et al. [8] the SINDy method is used to derive polynomial models for the lift of an airfoil.

In this paper, the Sparse Identification of Nonlinear Dynamics (SINDy) method [9] is applied to create accurate aerodynamic models of a simple flat plate subjected to airflow using data obtained from CFD (Computational Fluid Dynamics) simulations.

## Sparse Identification of Nonlinear Dynamics (SINDy)

In this paper, we use the Sparse Identification of Nonlinear Dynamical systems (SINDy) method, introduced by Brunton et al. [9, 10], and later refined in the work of Champion et al. [11]. An overview of the method and the description of the Python package that is used in our paper is given by Silva et al. [12]. Sparse Identification of Nonlinear Dynamics is a method based on representing the model as a system of possible nonlinear ordinary differential equations, whose right side can be written as a linear combination of some elementary functions [9]. Then a sparsity promoting regression is applied to determine the coefficients, resulting in easily interpretable models with only a few active terms. Physical constraints can be easily incorporated by constraining the regression procedure.

The LASSO and the STLSQ optimization method have been used for the regression. These methods have $l_1$ and $l_2$ regularized objective functions, respectively. The STLSQ procedure incorporates an adjustable threshold, any coefficient below this threshold is neglected. Then the regularization is repeated again for some iterations. The norms are defined as

$$l_1(\boldsymbol{x}) = \sum_{i=1}^{n} |x_i|, \tag{1}$$

$$l_2(\boldsymbol{x}) = \sqrt{\sum_{i=1}^{n} (x_i)^2}. \tag{2}$$

Using the formulas (1) and (2), the objective functions for the LASSO and STLSQ optimization procedure are respectively:

$$\frac{1}{2n} ||\boldsymbol{y} - \boldsymbol{X}\,\boldsymbol{w}||_2^2 + \lambda\, ||\boldsymbol{w}||_1\,, \tag{3}$$

$$\frac{1}{2n} ||\boldsymbol{y} - \boldsymbol{X}\,\boldsymbol{w}||_2^2 + \lambda\, ||\boldsymbol{w}||_2^2\,. \tag{4}$$

To determine the hyperparameters, the Optuna [13] package was used. Using this package, a multiobjective optimization was performed with the objectives defined as the error of the integrated model and the number of terms. So-called Pareto-optimal hyperparameter groups were determined. This means that for a given group, there are no other groups, which would result in an improvement over both objectives. This way, multiple models can be chosen, depending on the needs of the given task.

## Identified models

The CFD simulations that the models have been trained on were obtained by prescribing a sinusoidal oscillation for the pitch $(\alpha)$ or the plunge $(h)$ motion of the flat plate wing, with a 1m chord length. During the simulations we prescribed the motion in the following form

$$\alpha(t) = \alpha_{amp}\cos(\omega t), \qquad h(t) = h_{amp}\cos(\omega t), \tag{5}$$

where $\alpha_{amp}$ and $h_{amp}$ are the oscillation amplitudes, and $\omega$ is the angular frequency of the oscillation.
Data were obtained for three oscillation amplitudes and frequencies of the pitching and plunging motion, resulting in 18 different time series of the aerodynamic lift coefficient. The details of the CFD simulations are described in [14, 15].
Three models were identified, one for each frequency. The frequency was nondimensionalized; the resulting reduced frequency is defined as $k = \frac{\omega b}{U}$, where $b$ is the half chord length, $U$ is the wind velocity, and $\omega$ is the angular frequency of the oscillation.
The aerodynamic model equations were created by using the state variables $\alpha, \dot{\alpha}, C_{L_\alpha}, h, \dot{h}, C_{L_h}$. The Reduced-Order Models (ROMs) of the pitch $C_{L_\alpha}$ and the plunge $C_{L_h}$ induced lift coefficients are

$$\dot{C}_{L_\alpha}(\alpha, \dot{\alpha}, C_L; k) = a_1(k)\alpha + a_2(k)\dot{\alpha} + a_3(k)C_{L_\alpha} + a_4(k)\alpha^2 + a_5(k)\alpha\dot{\alpha}\ldots, \tag{6}$$

$$\dot{C}_{L_h}(h, \dot{h}, C_{L_h}; k) = b_1(k)h + b_2(k)\dot{h} + b_3(k)C_{L_h} + b_4(k)h^2 + b_5(k)h\dot{h}\ldots, \tag{7}$$

where a lexicographic ordering was used for the coefficients $a_i(k)$ and $b_i(k)$, which are listed in Table 1 and 2. We assume that the total lift coefficient $C_L$ is the sum of the pitch and the plunge induced lift coefficients, i.e.,

$$C_L = C_{L_\alpha} + C_{L_h}. \tag{8}$$

| Reduced frequency | $a_1$ | $a_2$ | $a_3$ | $a_{11}$ | $a_{16}$ | $a_{19}$ | $a_{35}$ | $a_{50}$ |
|---|---|---|---|---|---|---|---|---|
| $k = 0.1$ | 0.213 | 5.42 | 0 | 249 | 0 | 0 | -665.76 | -1.52·$10^6$ |
| $k = 0.2$ | 12.2 | 0 | -2.70 | 0 | 0 | 0.799 | 0 | 0 |
| $k = 0.5$ | 4.01 | 6.32 | -1.34 | 0 | -56.5 | 0.463 | 0 | 0 |

Table 1: The coefficients of the pitch reduced-order model (Eq. (6)).

| Reduced frequency | $b_1$ | $b_2$ | $b_3$ | $b_9$ | $b_{35}$ | $b_{50}$ |
|---|---|---|---|---|---|---|
| $k = 0.1$ | -0.172 | 2.874 | -0.398 | 0 | 0 | 0 |
| $k = 0.2$ | -0.715 | 2.33 | -0.34 | 0 | 0 | 0 |
| $k = 0.5$ | -6.47 | 6.43 | -1.6 | -0.033 | 14113 | 23599 |

Table 2: The coefficients of the plunge reduced-order model (Eq. (7)).

We determined the Normed Root Mean Squared Error (NRMS) of the aerodynamic models using the formula

$$\text{NRMS}_{C_L} = \frac{1}{C_{Lmax} - C_{Lmin}}\sqrt{\frac{\sum_{i=1}^{N}\left(C_L - \hat{C}_L\right)^2}{N}}, \tag{9}$$

where $N$ is the number of data points, $C_L$ is the CFD simulation data, $\hat{C}_L$, is the predicted value by the ROM simulation, $C_{Lmax}$ is the maximum, while $C_{Lmin}$ is the minimum value of the CFD simulation data. The NRMS for the three pitch and three plunge models can be found in Table 3 and 4, respectively.
For the reduced frequency $k = 0.1$, the lift coefficients from the CFD simulation and the fitted model as the a function of the angle of attack for oscillation amplitudes $\alpha_{amp} \in \{2°, 5°, 10°\}$ are shown in Figure 1.

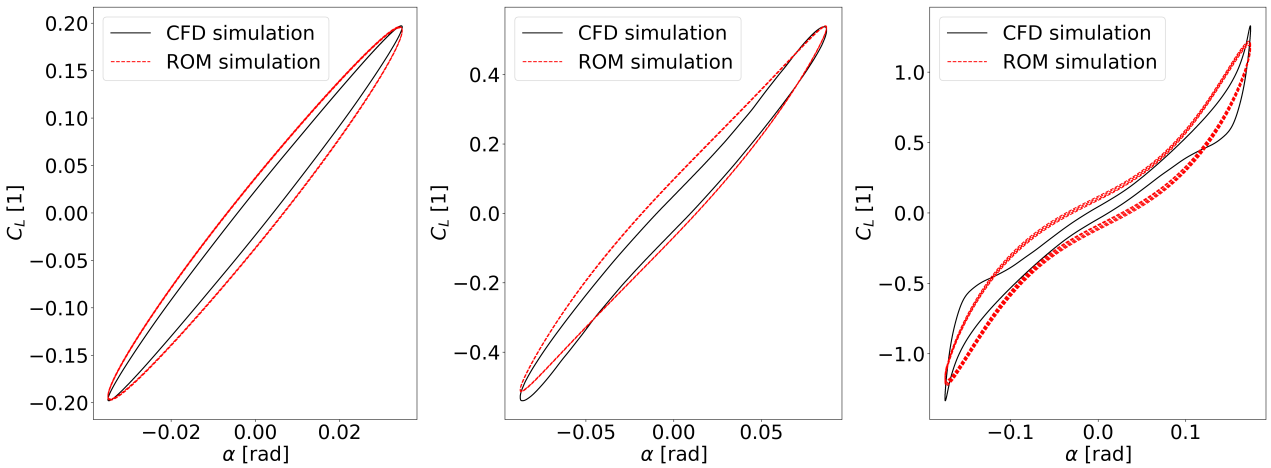


(a) $\alpha_{amp} = 2°$ (b) $\alpha_{amp} = 5°$ (c) $\alpha_{amp} = 10°$

Figure 1: Comparison of the identified ROM with the CFD simulation for $k = 0.1$ and $\alpha_{amp} \in \{2°, 5°, 10°\}$.

Figure 2 illustrates the comparison of the identified ROM with the CFD simulation for $k \in \{0.1, 0.2, 0.5\}$ and $\alpha_{amp} = 10°$. It can be observed that the models provide a very good fit overall, can reproduce the nonlinear behavior associated with the high angle of attack and high-frequency oscillations.

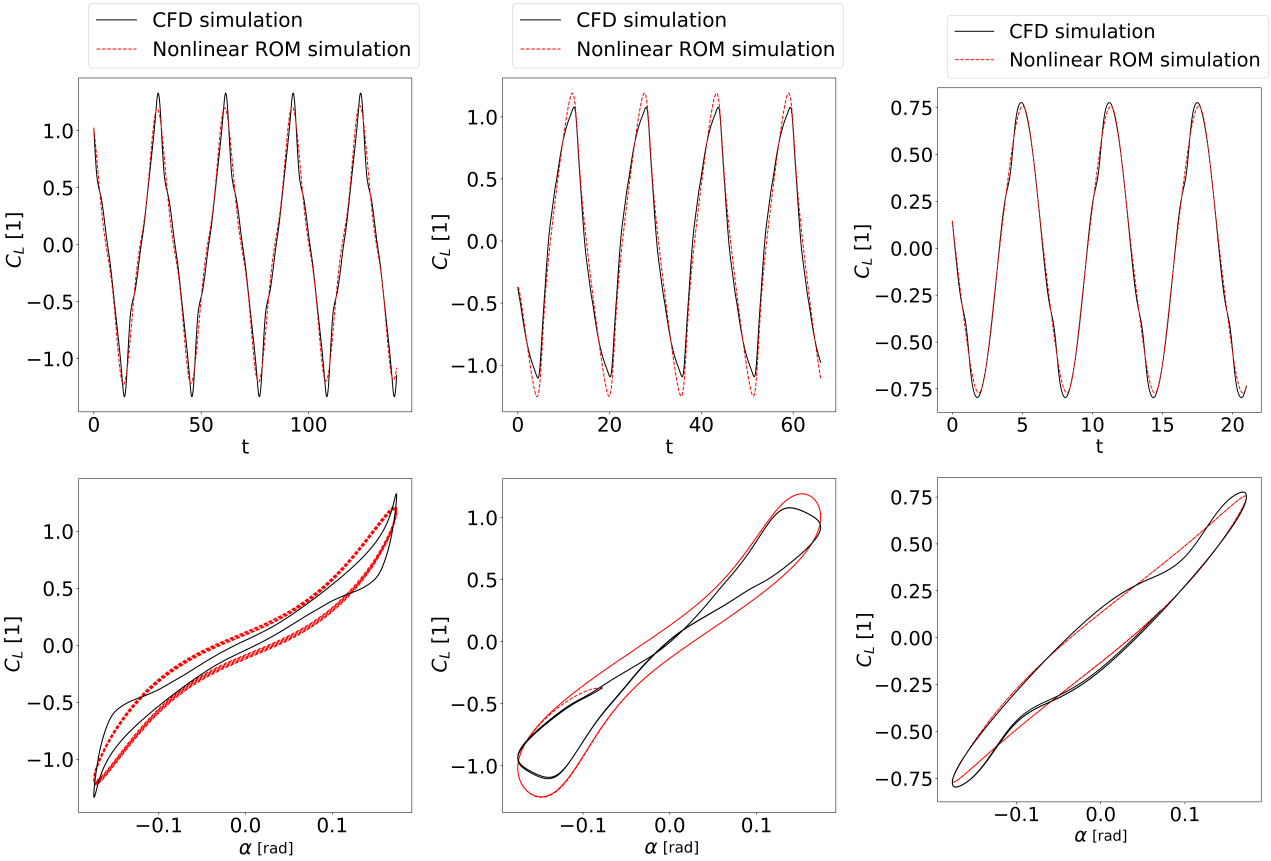


(a) $k = 0.1$ (b) $k = 0.2$ (c) $k = 0.5$

Figure 2: Comparison of the identified ROM with the CFD simulation for $k \in \{0.1, 0.2, 0.5\}$ and $\alpha_{amp} = 10°$.

For the reduced frequency $k = 0.1$, the lift coefficients from the CFD simulation and the fitted model as the a function of the plunge displacement for oscillation amplitudes $h_{amp} \in \{0.02\text{m}, 0.05\text{m}, 0.10\text{m}\}$ are shown in Figure 3. For the low reduced frequency $k = 0.1$, the reduced-order model gives an almost perfect fit.

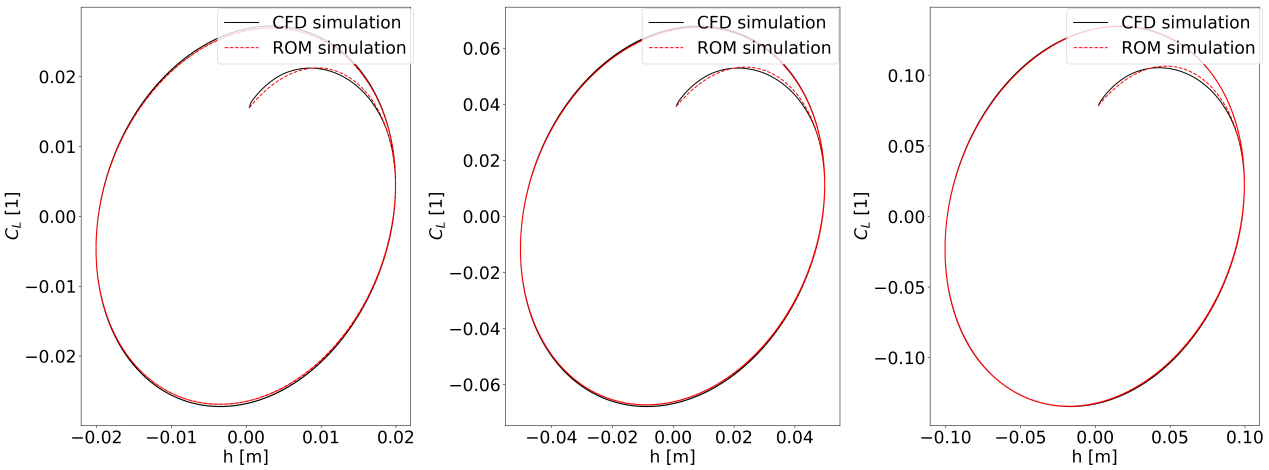


(a) $h_{amp} = 0.02\text{m}$ (b) $h_{amp} = 0.05\text{m}$ (c) $h_{amp} = 0.10\text{m}$

Figure 3: Comparison of the identified ROM with the CFD simulation for $k = 0.1$ and $h_{amp} \in \{0.02\text{m}, 0.05\text{m}, 0.10\text{m}\}$.

Figure 4 illustrates the comparison of the identified ROM with the CFD simulation for $k \in \{0.1, 0.2, 0.5\}$ and plunge amplitudes $h_{amp} = 0.1\text{m}$. It can be observed that the models provide a very good fit overall, can reproduce the nonlinear behavior associated with the high plunge amplitudes and high-frequency oscillations.

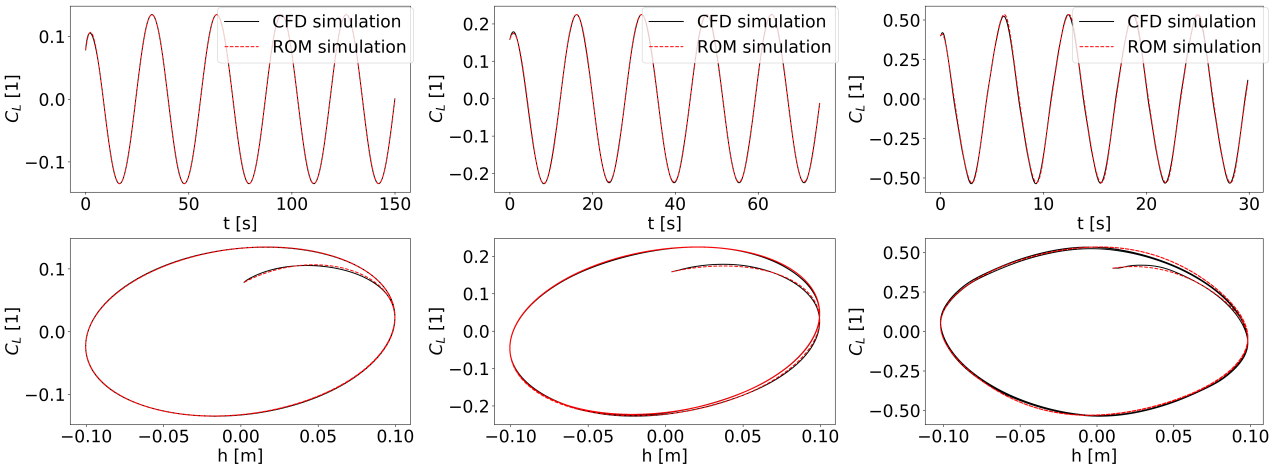


(a) $k = 0.1$ (b) $k = 0.2$ (c) $k = 0.5$

Figure 4: Comparison of the identified ROM with the CFD simulation for $k \in \{0.1, 0.2, 0.5\}$ and $h_{amp} = 0.10\text{m}$.

| Oscillation amplitude | Model for $k = 0.1$ | Model for $k = 0.2$ | Model for $k = 0.5$ |
|---|---|---|---|
| $2°$ | 2.53% | 1.88% | 1.66% |
| $5°$ | 2.45% | 2.25% | 0.94% |
| $10°$ | 3.44% | 4.62% | 1.61% |

Table 3: The NRMS values of the identified aerodynamic models for the pitching motion.

| Oscillation amplitude | Model for $k = 0.1$ | Model for $k = 0.2$ | Model for $k = 0.5$ |
|---|---|---|---|
| 0.02m | 0.46% | 0.67% | 4.73% |
| 0.05m | 0.4% | 0.65% | 4.13% |
| 0.10m | 0.36% | 0.65% | 0.89% |

Table 4: The NRMS values of the identified plunge aerodynamic models.

### Performance of the models for coupled pitch and plunge motions

To check the accuracy of the identified models, we have run coupled pitch and plunge motion simulations. We defined the following coupled motion

$$\alpha(t) = \alpha_{amp}\cos(\omega t), \qquad h(t) = h_{amp}\cos(\omega t + \phi), \tag{10}$$

where $\phi$ is the phase between the motions of the pitch and plunge.
In Figure 5 the comparison is shown between the CFD simulation, and the identified ROM model for $k = 0.1$, $\alpha_{amp} = 10^\circ$, and $h_{amp} = 0.1$m for three different phase shift values. Both the combined pitch-plunge model and also the pitch-only model is shown. It can be observed that the combined model can capture the nonlinear aerodynamic forces for the coupled pitch and plunge motion. Using the combined model, the error in the maximum value of the lift is reduced by up to 87%. The NRMS values of the combined model for the three test cases were under 5%.

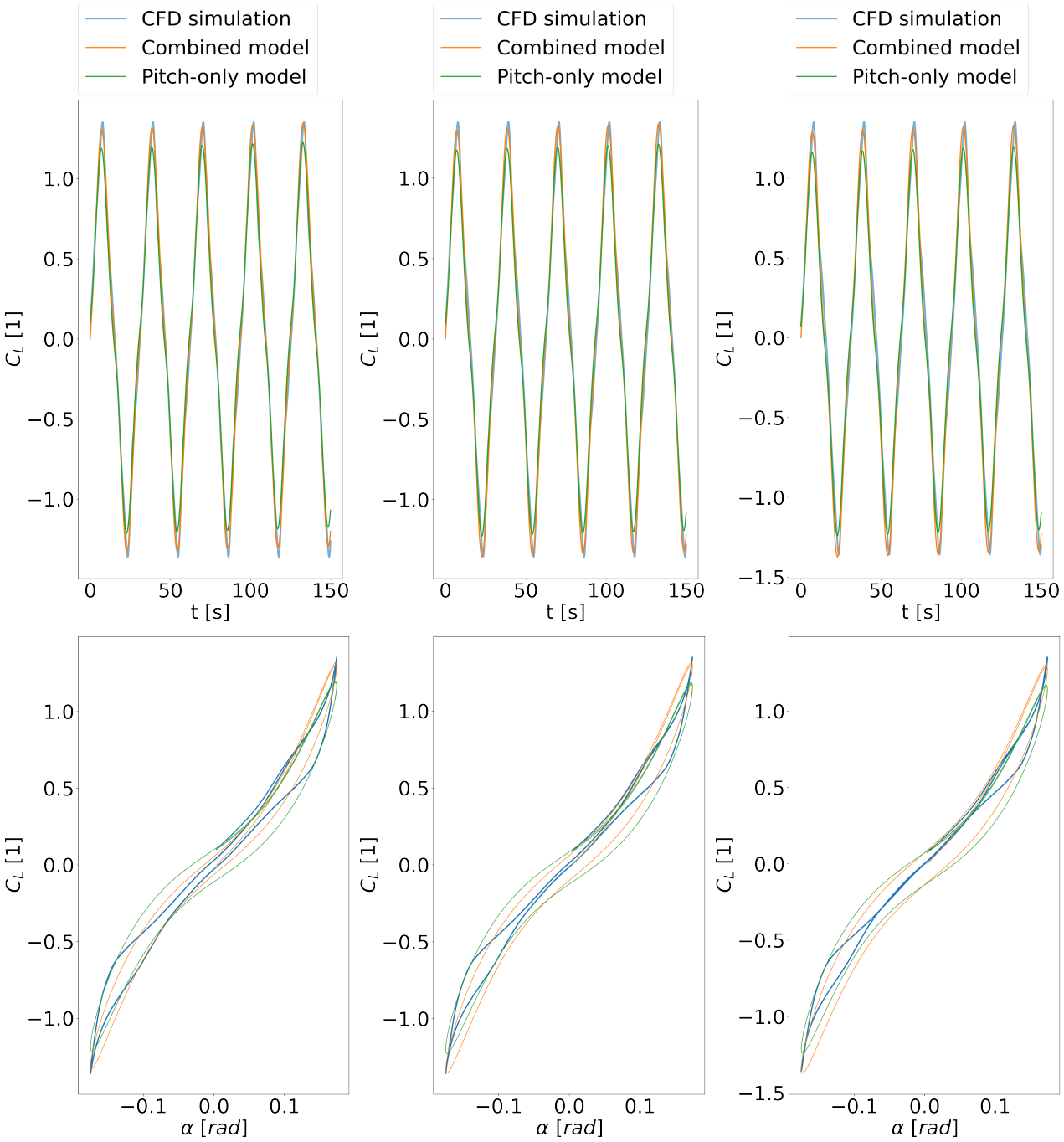


(a) $\phi = 80^\circ$ (b) $\phi = 90^\circ$ (c) $\phi = 100^\circ$

Figure 5: Comparison of the identified ROM with the CFD simulation for $k = 0.1$, $\alpha_{amp} = 10^\circ$, and $h_{amp} = 0.1$m.

## Conclusions

The significant problem of creating reduced-order models for aerodynamic loads, valid for large amplitude, and frequency oscillations, was studied. The SINDy method was utilized to extract the governing differential equation of the aerodynamic lift coefficient from CFD data of a flat plate with pitching and plunging motion. This method resulted in easily interpretable, simple models. It was shown that the identified models for one particular frequency show excellent agreement with the CFD simulation data for varying amplitude oscillations. The future goal of this research is to couple the created aerodynamic model to the structural dynamical model of a flexible plate subjected to airflow.

## Acknowledgements

The research reported in this paper and carried out at the Budapest University of Technology and Economics has been supported by the ÚNKP-21-3 New National Excellence Program of the Ministry for Innovation and Technology (ITM) of Hungary from the source of the National Research Development and Innovation Fund, and the NRDI Funds (TKP2020 National Challenges Subprogram, Grant No. BME-NCS) based on the charter of bolster issued by the NRDI Office under the auspices of the ITM. The research reported in this paper is part of project no. BME-NVA-02, implemented with the support provided by the ITM of Hungary from the NRDI Fund, financed under the TKP2021 funding scheme. This work has been supported by the Hungarian NRDI Fund under contract NKFI K 137726.

## References

[1] Holierhoek, J., De Vaal, J., Van Zuijlen, A., and Bijl, H. (2013). Comparing different dynamic stall models. *Wind Energy*, 16(1):139–158.

[2] Fonzi, N., Brunton, S. L., and Fasel, U. (2020). Data-driven nonlinear aeroelastic models of morphing wings for control. *Proceedings of the Royal Society A*, 476(2239):20200079.

[3] Li, S., Kaiser, E., Laima, S., Li, H., Brunton, S. L., and Kutz, J. N. (2019). Discovering time-varying aerodynamics of a prototype bridge by sparse identification of nonlinear dynamical systems. *Physical Review E*, 100(2):022220.

[4] Boutet, J. and Dimitriadis, G. (2018). Unsteady lifting line theory using the wagner function for the aerodynamic and aeroelastic modeling of 3d wings. *Aerospace*, 5(3):92.

[5] Lelkes, J. and Kalmár-Nagy, T. (2021). Analysis of a piecewise linear aeroelastic system with and without tuned vibration absorber. *Nonlinear Dynamics*, 103(4):2997–3018.

[6] Sun, C., Tian, T., Zhu, X., and Du, Z. (2020). Sparse identification of nonlinear unsteady aerodynamics of the oscillating airfoil. *Proceedings of the Institution of Mechanical Engineers, Part G: Journal of Aerospace Engineering*, 235(7):809–824.

[7] Brunton, S. L., Kutz, J. N., Manohar, K., Aravkin, A. Y., Morgansen, K., Klemisch, J., Goebel, N., Buttrick, J., Poskin, J., Blom-Schieber, A. W., and et al. (2021). Data-driven aerospace engineering: Reframing the industry with machine learning. *AIAA Journal*, page 1–26.

[8] Pohl, J., Semaan, R., and Jones, A. R. (2019). Dynamic lift measurements on an airfoil with periodic flap motion at high reynolds number. *AIAA Scitech 2019 Forum*.

[9] Brunton, S. L., Proctor, J. L., and Kutz, J. N. (2016). Discovering governing equations from data by sparse identification of nonlinear dynamical systems. *Proceedings of the National Academy of Sciences*, 113(15):3932–3937.

[10] Brunton, S. L., Proctor, J. L., and Kutz, J. N. (2016). Sparse identification of nonlinear dynamics with control (sindyc). *IFAC-PapersOnLine*, 49(18):710–715.

[11] Champion, K., Zheng, P., Aravkin, A. Y., Brunton, S. L., and Kutz, J. N. (2020). A unified sparse optimization framework to learn parsimonious physics-informed models from data. *IEEE Access*, 8:169259–169271.

[12] Silva, B. D., Champion, K., Quade, M., Loiseau, J.-C., Kutz, J., and Brunton, S. (2020). Pysindy: A python package for the sparse identification of nonlinear dynamical systems from data. *Journal of Open Source Software*, 5(49):2104.

[13] Akiba, T., Sano, S., Yanase, T., Ohta, T., and Koyama, M. (2019). Optuna. *Proceedings of the 25th ACM SIGKDD International Conference on Knowledge Discovery & Data Mining*.

[14] Lendvai, B. and Lelkes, J. (2021). Aeroelasztikus szárnymodell numerikus vizsgálata: Numerical analysis of aeroelastic wing model. *Nemzetközi Gépészeti Konferencia–OGÉT*, pages 48–51.

[15] Lelkes, J. and Lendvai, B. (2021). Torziós csillapító alkalmazása belebegés megszüntetésére: Application of a torsional absorber for flutter suppression. *Nemzetközi Gépészeti Konferencia–OGÉT*, pages 44–47.